

Analysis of the APR1400 PWR Initial Core with the nTRACER Direct Whole Core Calculation Code and the McCARD Monte Carlo Code

Hyunsik Hong and Han Gyu Joo*

Department of Nuclear Engineering, Seoul National University, 1 Gwanak-gu, Seoul, Korea

*Corresponding author: joohan@snu.ac.kr

1. Introduction

The remarkable growth of computing power nowadays makes high-fidelity reactor core calculations more feasible and institutions worldwide have put their effort on the development of advanced code systems. A direct whole core calculation code nTRACER [1] being developed in Seoul National University (SNU) is one of the leading codes. By employing the 2D/1D approach, which utilizes the method of characteristics (MOC) for radial two-dimensional (2-D) calculation and the simplified P3 (SP3) source expansion nodal method (SENM) for axial one-dimensional calculation, and using three-dimensional (3-D) coarse mesh finite difference (CMFD) method to accelerate the solution convergence, nTRACER can perform high-fidelity direct whole core calculation within practical computing time limits.

Efforts to validate the solution capability of nTRACER have been made consistently. The code has already been applied to the core follow calculations of two Korean OPR1000 pressurized water reactor (PWR) cores, Yonggwang Nuclear Unit 3 and Ulchin Nuclear Unit 5, and to the realistic core benchmark calculations such as BEAVRS [2] and VERA [3]. However, the cores being analyzed through previous studies are in the generation II reactor group whose core is not challenging enough to test the capability of the advanced codes. For this reason, the analysis of the APR1400 PWR core, which is one of the generation III reactors, has been started.

This paper presents the modeling approach of the APR1400 PWR initial core and hot-zero-power (HZIP) solutions of the models at various scales. The specification of the nTRACER core model is described as detailed as possible without the proprietary information. The validity of modeling and the solution accuracy are assessed by the comparisons with the solutions of the McCARD continuous energy Monte-Carlo code of SNU [4].

2. APR1400 PWR Core Models

The Advanced Power Reactor (APR) 1400 PWR designed by KEPSCO/KHNP is one of the generation III reactors. It is developed from Optimized Power Reactor (OPR) 1000 and incorporates features from Combustion Engineering System 80+ design [5].

Its initial core designed to yield 4000 MW thermal power to generate 1400 MW electric power has 241 fuel

assemblies loaded in 17x17 core array [6]. The assemblies having 16x16 lattice feature with 236 fuel rods and 5 guide tubes are categorized into three types, A, B and C, by enrichment of the fuel. Note that the fuel rods except for the lowest one have lower enriched part that are called cutback at the top and bottom. The assemblies commonly have top and bottom grids made of Inconel and nine intermediate grids made of ZIRLO. The assemblies in B and C types are subdivided by loading pattern of the fuel rods and the number of burnable poison (BP) rods. Those also have enrichment zoning which is formed by placing lower enriched fuel pins near the guide tubes and inter-assembly water gap between the neighboring assemblies.

To control excessive reactivity of the robust initial core, Gadolinia bearing BP pins are loaded in the selected assemblies. The BP and fuel pins have the same dimensions but the BP pellet is made of $Gd_2O_3-UO_2$ mixture except for the top and bottom cutback parts which are filled with un-poisoned UO_2 pellet to prevent unnecessary suppression of the neutron flux on the low powered region. Two types of control element assembly (CEA), the full and part-strength, are also used to the core control. The full-strength CEAs consists of either four or twelve control rods bearing boron carbide (B4C) absorber in Inconel 625 tubing. Those are used in five regulating groups and two shutdown groups. The part strength CEAs have four control rods per each and the absorber material is the same with the tubing.

The core is surrounded by stainless steel shroud, core support barrel, and reactor vessel.

2.1 The nTRACER Model

The modeling was started from a fuel pin level. The fuel pin cell including UO_2 pellet, air gap, cladding and coolant were explicitly modeled. To properly consider sub-pin level flux variations, the fuel pellet region was subdivided into 40 regions by five annular rings and eight azimuthal sectors, and the moderator region was subdivided into 32 regions by four annular rings and 8 azimuthal sectors. Note that the number of subdivisions in the BP pellet is 80, doubling that of the fuel pellet, because of the large cross section of Gadolinia. The two Inconel grids and nine ZIRLO grids were semi-explicitly modeled by placing the grid material in the corners of a cell, as shown in Fig. 1 with the subdivisions in a normal fuel pin cell, by preserving total area of dark blue colored region in the left side.

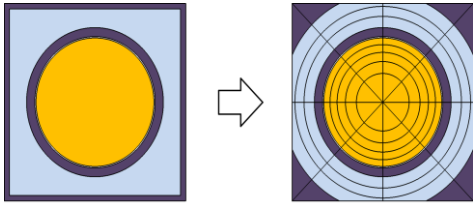


Fig. 1. Fuel pin cell model of the nTRACER with the semi-explicitly modeled spacer grid and the sub-pin regions

The fuel assembly was made by loading the fuel and BP pin models and five guide tubes which have four pin cell space per each. The assembly water gaps were also modeled explicitly. Axial structure of the assemblies was subdivided into 36 planes; the explicitly modeled 33 planes were in the active core region with fuel and the remaining were the homogenized structure and reflectors on the top and bottom of the active core.

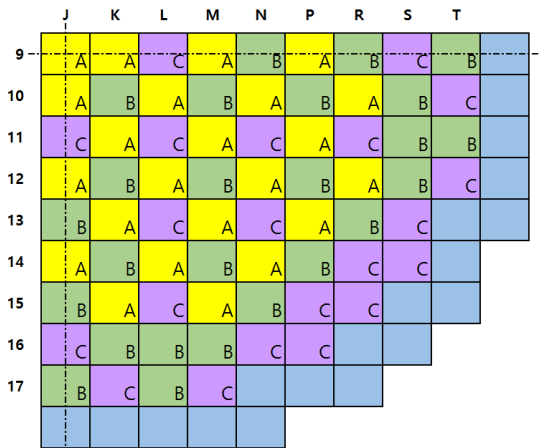


Fig. 2. Radial configuration of the nTRACER quarter core model with surrounding assembly-sized reflector

241 fuel assemblies were loaded in a 17x17 array like in Fig. 2 that shows a quadrant. The fuel region of the core was surrounded by an assembly-thick reflector which includes stainless steel shroud and moderator filling the gap and outside of the shroud. Other structures such as core vessel was not modeled. The quarter core nTRACER model employed the reflective boundary condition set on the center line on the row 9 and column J, shown by dotted lines in the figure.

2.2 The McCARD Model

The McCARD models were prepared in the same time to generate Monte-Carlo solutions to be used in the assessment of corresponding nTRACER solutions.

Basically, the McCARD models were nearly the same with the nTRACER model. The core constituents, such as the fuel pin, BP pin, guide tubes, and the water gap, were modeled explicitly. The axial geometry was the same also to make ease comparison between the codes. The only difference was the spacer grid modeling shown in Fig. 1. Compare to the nTRACER model which have

four corners filled with the grid material, the McCARD model had box-shaped grid sleeves placed at the four-sides of the pin cell.

3. Calculated Results and Assessment

The 47-group nTRACER library and the continuous energy McCARD library were used for the calculations to be reported below. Both libraries were generated from ENDF/B-VII.0 data. The calculations were carried out on a LINUX cluster composed of 21 nodes with dual mounted 2.67GHz Intel Xeon X5650 hexa-core processors and 12 nodes with dual mounted 2.60GHz Intel Xeon E5-2650 v2 octa-core processors.

The nTRACER calculations were performed with the ray spacing of 0.05cm and 16/4 azimuthal/polar angles in the octant of the solid angle sphere, and P2 scattering MOC solver [7] was used unless otherwise noted.

3.1 Two-dimensional Lattices

Comparison between the nTRACER and McCARD was made from the lattices which represent mid-plane of the fuel assemblies. The results are in Table I.

The table shows k-effective yielded by MC and NT, which denote McCARD and nTRACER, and reactivity difference and absolute pin power error of the two. RMS and Max indicate root-mean-square and the maximum value of the error. Note that the McCARD calculations were performed with 500,000 particles per cycle and 100/500 inactive/active cycles. Standard deviation (StDev) of the k-effective was about 4 pcm. Relative pin power error is not included in the table because the BP pin always shows the Max larger than 1.0% due to its low power.

Agreement between the McCARD and nTRACER was good for both k-effective and pin power distribution. Underestimation of k-effective was large in A0 lattice case with the lowest enriched fuel but the difference was less than 200 pcm. Absolute pin power error was within 0.5% for all the lattices.

Table I: Results of the 2-D lattices

ID	McCARD	nTRACER			
	k-eff	k-eff	$\Delta\rho$ (pcm)	Pin Err. RMS	Pin Err. Max
A0	1.09912	1.09694	-181	0.10%	0.24%
B0	1.28687	1.28559	-77	0.13%	0.33%
B1	1.09100	1.09051	-41	0.16%	0.38%
B2	1.07805	1.07742	-54	0.16%	0.39%
B3	1.03736	1.03728	-7	0.19%	0.48%
C0	1.31321	1.31206	-67	0.14%	0.34%
C1	1.13760	1.13723	-29	0.16%	0.40%
C2	1.08708	1.08712	3	0.19%	0.47%
C3	1.07747	1.07746	-1	0.19%	0.47%

3.2 Two-dimensional Core

The 2-D core represents the radial slice of axial mid-plane of the core. Similar with the lattices, k-effective and assembly-wise power distribution were compared on it. The nTRACER calculations were performed with not only the P2 but also the P1 MOC solver, and the McCARD calculation was performed with two million of particles per cycle and 500/500 inactive/active cycles. StDev of the k-effective was about 2 pcm. The results are in Table II and Fig. 3. Note that the figure shows not a quadrant but an octant.

Table II: Results of the 2-D core

Code	k-eff	$\Delta\rho$ (pcm)	ASM Err. RMS	ASM Err. Max
McCARD	1.00196	-	-	-
nT, P1	1.00028	-168	0.87%	1.48%
nT, P2	1.00105	-91	1.59%	2.55%

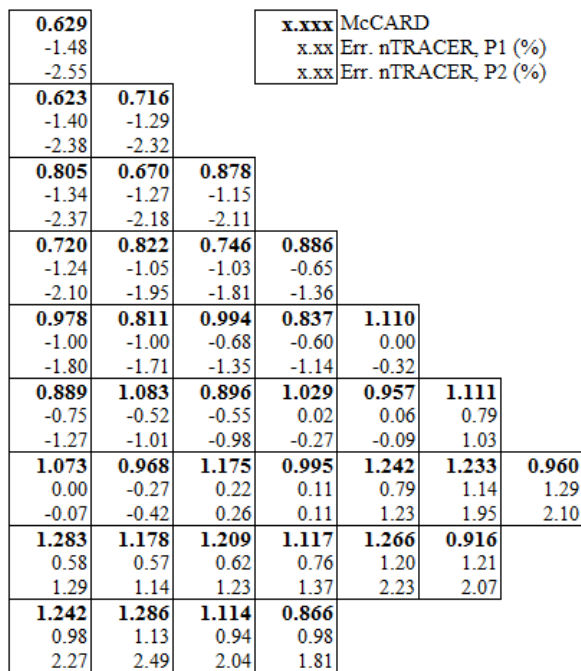


Fig. 3. Assembly power and absolute error distributions in an octant of the core

As shown in Table II, discrepancy between the nTRACER and McCARD was significant in both the reactivity and the power distribution. Underestimation of the k-effective was larger than 100 pcm in the P1 case but decreased within 100 pcm in the P2 case.

More remarkable one was the power distribution shown in Fig. 3. The figure showed that the error was large and moreover, there was a certain tendency on its distribution. In the P1 case, for example, the power was overestimated about 1.3% at the core periphery and underestimated about 1.5% at the core center. The error got larger in the P2 case. This tendency made in-out

tilted feature on the global error distribution. Currently, study on the tilted power distribution is being performed and not the code itself but the library is suspected as the reason of the problem.

3.3 Three-dimensional Single Assembly

The 3-D assemblies were prepared as an expanded version of the 2-D lattices. Boundary conditions were the vacuum at the top and bottom and the reflective at the four other sides. As written in modeling descriptions, axial geometry of the nTRACER single assembly models was composed of 33 active fuel planes and 3 non-fuel structure planes. Note that the plane or the axial plane to be mentioned below denotes a radially averaged plane which represents one of the 33 active fuel planes. The McCARD models were made nearly the same with the nTRACER and the McCARD calculations were performed with two million particles per cycle and 500/500 inactive/active cycles. StDev of the k-effective was about 2 pcm.

The results are in Table III. Plane Err. which means absolute error in radially averaged axial power is in the table instead of the absolute pin power error because the error was within 0.4% for all the cases.

Table III: Results of the 3-D lattices

ID	McCARD	nTRACER			
	k-eff	k-eff	$\Delta\rho$ (pcm)	Plane Err. RMS	Plane Err. Max
A0	0.99574	0.99420	-156	0.29%	0.63%
B0	1.19049	1.18975	-52	0.17%	0.38%
B1	1.01546	1.01555	9	0.53%	0.72%
B2	1.00399	1.00402	3	0.37%	0.58%
B3	0.96784	0.96801	19	0.37%	0.70%
C0	1.22202	1.22146	-37	0.19%	0.32%
C1	1.06459	1.06481	19	0.37%	0.66%
C2	1.01934	1.01963	28	0.35%	0.60%
C3	1.00883	1.00908	25	0.13%	0.50%

Agreements between the nTRACER and McCARD were good in general. The nTRACER underpredicted the k-effective in the assemblies with the low enriched fuel but the reactivity difference was within 200 pcm. The axial power distribution, meanwhile, was good with no exception because application of the enrichment zoning and BP do not pose significant increase in axial heterogeneity of the core. Fig. 4. shows axial power and error distribution of C3 assembly which have both the enrichment zoning and BP pins. In the figure, the step line which corresponds to the nTRACER completely overlapped the McCARD line.

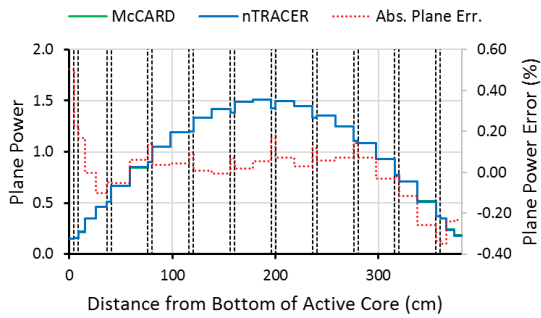


Fig. 4. Axial power and absolute error distribution of C3 3-D single assembly

3.4 Three-dimensional Core

It would be desirable to compare both the k -effective and power distribution of the core for the thorough comparisons but reliable Monte-Carlo solution on the power could not be obtained yet due to excessively large computing time to be required. For this reason, only the k -effective comparisons were made on the core at all-rod-out (ARO) state first.

On the ARO core, the McCARD calculation was performed with a million particles per cycle and 500/500 inactive/active cycles. StDev of the k -eff is about 3 pcm. The result was not satisfactory. The k -effective yielded by the nTRACER and McCARD were 1.00161 and 1.00007 so the reactivity difference was -154 pcm; the large difference like the 2-D core.

After the calculation at ARO state had been finished, the full-strength CEAs were inserted in the core. The McCARD calculation was performed by using 200,000 particles per cycle and 500/500 inactive/active cycles. The results are in Table IV. Grp. and Acc. denote group worth and accumulated worth.

Table IV: Results of the rod worth calculations

ID	McCARD		nTRACER		Diff.	
	Grp. (pcm)	Acc. (pcm)	Grp. (pcm)	Acc. (pcm)	Grp. (%)	Acc. (%)
5	258	258	267	267	3.4	3.4
4	422	680	411	678	-2.6	-0.3
3	661	1341	666	1344	0.8	0.2
2	920	2261	906	2250	-1.5	-0.5
1	1130	3391	1158	3408	2.5	0.5
B	4774	8165	4762	8171	-0.2	0.1
A	5748	13913	5719	13890	-0.5	-0.2

The reactivity difference attributed by full insertion of a CEA insertion was assumed as worth. The worth gained by all the inserted CEAs was assumed as accumulated worth and the reactivity difference of a certain state and the previous state was assumed as group worth. Agreement between the nTRACER and McCARD was good in all the cases.

4. Summary and Conclusions

The nTRACER model of the APR1400 PWR initial core was established and the validity of the modeling was confirmed through a series of HZP comparisons with the Monte-Carlo solutions of McCARD code. Most of the core constituents including fuel and BP pins, guide tubes, and spacer grids were explicitly modeled.

The comparisons not only confirmed the validity but also showed the current problems of the nTRACER. In the lattice and assembly cases, agreement between the two codes was good in prediction of the k -effective and radial and axial power distributions. The absolute error in the radial pin power and axial plane power distributions were within 0.5% and 0.8%, respectively, and except for A0 assembly with the lowest enrichment, the reactivity difference was less than 100 pcm. Agreement was also satisfactory in the rod worth calculations. However, in the 2-D and 3-D core cases, the nTRACER yielded significant amount of error for the k -effective and radial power distribution. The reactivity difference was larger than 100 pcm in the P1 of the 2-D core and the 3-D core at ARO state. Significant under- and over-estimation of the fission power at the core center and periphery were also worthwhile to be noted.

Through this work, the solution capability of nTRACER could be tested and the bases for further studies were successfully prepared. Calculations under the hot-full-power and depleted core is now underway.

REFERENCES

- [1] Y. S. Jung, H. G. Joo et al., Practical Numerical Reactor Employing Direct Whole Core Neutron Transport and Subchannel thermal/hydraulic solvers, *Annals of Nuclear Energy*, Vol. 62, pp. 357-374, 2013
- [2] M. Ryu, H. G. Joo et al., Solution of the BEAVRS benchmark using the nTRACER direct whole core calculation code, *Journal of Nuclear Science and Technology*, Vol. 52, pp.961-969, 2014
- [3] M. Ryu, H. G. Joo et al., Preliminary Assessment of nTRACER and McCARD Direct Whole Core Transport Solutions to VERA Core Physics Benchmark Problems, *Transaction of the American Nuclear Society* 111:1244-1247, Jan. 2014
- [4] B. S. Han, H. J. Shim et al., McCARD: Monte Carlo Code for Advanced Reactor Design and Analysis, *Nuclear Engineering and Technology*, Vol. 44, pp.151-176, 2012
- [5] S. Goldberg, R. Rosner, *Nuclear Reactors: Generation to Generation*, American Academy of Arts and Sciences, pp. 7-20, 2011
- [6] S. S. Lee, S. H. Kim et al., The Design Features of the Advanced Power Reactor 1400, *Nuclear Engineering and Technology*, Vol. 41, pp. 995-1004, 2014
- [7] M. Ryu, H. G. Joo et al., Incorporation of Anisotropic Scattering in nTRACER, *Trans. of Korean Nuclear Society*, Pyeong-chang, Oct. 27-31, 2014